Spectrochimica Acta Part A: Molecular and Biomolecular Spectroscopy 302 (2023) 123067

Contents lists available at ScienceDirect

Spectrochimica Acta Part A:
Molecular and Biomolecular Spectroscopy

journal homepage: www.journals.elsevier.com/spectrochimica-acta-part-a-molecular-and-biomolecular-spectroscopy

Enhancement of protein detection on cultural heritage samples after SYPRO™ Ruby staining by optical microscopy and micro-FTIR spectroscopy

M. Botticelli [a], V. Risdonne [a,b], C. Young [a,*]

[a] Kelvin Centre for Conservation and Cultural Heritage Research, University of Glasgow, Kelvin Hall, 1445 Argyle Street, Glasgow G3 8AW, UK
[b] Science Lab, Collections Care and Access, Victoria & Albert Museum, South Kensington, Cromwell Road, London SW7 2RL, UK

HIGHLIGHTS

- Detection of protein layers in artworks was studied using staining and μ-FTIR;
- Mock-ups with animal glue and samples from case studies were analysed;
- The staining validates protein mapping with external reflection μ-FTIR;
- Protein band position varies when inorganic/organic compounds are present;
- Staining with μ-FTIR mapping highlights protein distribution in multi-layer samples.

GRAPHICAL ABSTRACT

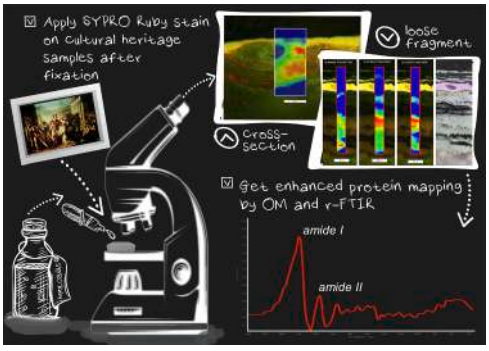

ARTICLE INFO

Keywords:
Fluorescent staining tests
Protein detection
Optical microscopy
external reflection micro-FTIR
Painting cross-sections

ABSTRACT

The paper investigates SYPRO™ Ruby staining in combination with external reflection micro-FTIR spectroscopy, for the detection of proteinaceous media in paint layers on cultural heritage, from unembedded micro-fragments and samples embedded in cross-sections. Combining FTIR spectroscopy with staining helped to verify that the FTIR mapping is accurate when performed by the integration of the main amide I and II bands, despite their naturally occurrent distortions due to the specular component and material absorption/surface properties. The research filled some gaps in the published literature on SYPRO™ Ruby interaction with different Cultural Heritage materials, including identifying drawbacks, e.g. swelling mechanisms in the sample after staining. The effects of the staining were investigated on different reference samples containing rabbit skin glue (proteinaceous), and samples from cultural heritage case studies undergoing technical examination as part of research projects, where identification of protein is an important aspect of understanding the sequence of complex multi-layers within a sample. Results showed that, when external reflection μ-FTIR is performed after the staining, the contribution from amide I and II, which occurs at higher wavenumbers than in transmission or attenuated total reflection, is more resolved and therefore easier to determine. When inorganic or organic compounds are present in the same layer, variation in the position of amide bands can occur. However, they can be used for chemical mapping using simple data-treatment strategies, as validated with the positive staining. This type of data

* Corresponding author.
E-mail address: christina.young@glasgow.ac.uk (C. Young).

https://doi.org/10.1016/j.saa.2023.123067
Received 10 March 2023; Received in revised form 4 May 2023; Accepted 20 June 2023
Available online 22 June 2023

processing gives a good estimation of the protein distribution in the layers, both in terms of morphology and thickness, on mock-up samples and cross-sections from real case studies.

1. Aims of the research

The research objective was to verify that the complementary techniques of external reflection micro-FTIR (henceforth μ-FTIR) and staining produce results which corroborate each other, mitigating the limitations of each technique. The literature on SYPRO™ Ruby metal-chelate stain was re-evaluated and the effect of its application on proteinaceous media typically found in cultural heritage samples was assessed using the combination with optical microscopy (OM) and μ-FTIR spectroscopy. It is still common practice among conservators and conservation scientists to study micro-samples using cross-sections embedded in various resins, all of which have IR signals that interfere with the identification of media. The combined techniques were applied to mock-up and case-study samples to determine whether the drawbacks of each technique could be mitigated: μ-FTIR can help determine if the interaction of a sample with the staining solution produces a chemical change or swelling mechanism; the staining images can verify the FTIR mapping; the comparison of staining images and FTIR maps also help to identify any potential interference from other compounds in the protein-based layer or neighbouring layers of the cross-section. The staining can also show when μ-FTIR mapping is not affected by spectral distortions (naturally occurring in external reflection because of different material absorption/surface properties and the interaction of the sample with the radiation). The comparison of staining and μ-FTIR is also aimed at providing preliminary guidelines on how to combine them with the best data-processing strategy for the mapping of protein in different types of sample: loose or embedded, porous or compact. Understanding the interaction of the staining solution with protein in simple or more complex multi-layered systems will help in the definition of criteria for protein detection in cultural heritage materials.

2. Introduction

2.1. Protein detection in works of art

The current practice used by many conservators and conservation scientists of analysing paint samples as cross-sections using optical microscopy in the visible and UV regions requires casting samples in polyester or epoxy resins, followed by polishing. Cross-sections retain the stratigraphy of the sample and allow for both visual pigment identification, indication of the technique e.g. wet in wet painting and, when combined with staining, of the media in the various layers. The complementary technique of Fourier-transform infrared spectroscopy (FTIR) is well-established (not always available to conservators) and is used to characterise organic and inorganic painting materials in artworks [1–5]. It is also suitable more generally for cultural heritage research because it is a fast technique requiring minimum sample preparation and in most configurations does not destroy the sample. The use of different instrumental setups, i.e. attenuated total reflectance (ATR-FTIR), diffuse reflectance infrared Fourier transform spectroscopy (DRIFT), photoacoustic spectroscopy (FTIR-PAS), micro-FTIR spectroscopy, makes it versatile for the investigation of both organic and inorganic materials [6]. It can be applied to small objects or parts of larger objects with no sample removal [7] or multi-layered cross-sections [8,9]. These techniques are the focus and application of our research. Embedding media are characterised by several FTIR peaks in the 3000–2800 cm^{-1} and 1800–1100 cm^{-1} regions, where traditional and modern painting media in the preparation and paint layers have their fingerprint signals. Therefore, the presence of the casting resin mostly impedes, or at least complicates, the identification and discrimination of organic components in the layers [10,11]. Trying to remove the contribution of the casting resin from the spectra or from an absorbance map, for example by subtracting or deconvolving the reference spectrum of the casting resin is not the best solution. This is because the operation can remove some of the overlapping peaks that belong to the sample itself.

Ideally, it would be preferrable to analyse an untreated sample. However, to define and analyse its stratigraphy with micro-FTIR, a flat surface must be placed perpendicular to the irradiating IR beam and be within the depth of field of the microscope (over the area of interest). Hand polishing a loose sample to achieve this flat surface is only possible if a generous size of the sample is available, and it can be safely held in a support that holds the sample in position without damage. This is rarely an option for samples from cultural heritage objects.

Recently, alternative casting methods have been explored using KBr/NaCl embedding [12,13] or cyclododecane coating prior to resin embedding [10,11]. These samples have been analysed by ATR-FTIR, a technique that offers rapid acquisition, good reproducibility and high quality. Very good contact between the sample and ATR crystal is essential for high signal-to-noise results [14]. This requirement cannot be ensured when loose samples are analysed, especially if they are prone to crumble, or when the sample in the cross-section makes it difficult to achieve a smooth polished and flat surface.

An alternative FTIR configuration allows investigation of the composition of a sample without direct contact and possible damage by using μ-FTIR. This configuration has been applied on solid samples, either for surface inspection by point analysis or chemical mapping on cross-sections [15,16]. When the IR beam interacts with the sample in external reflection, both surface and volume interactions occur [14]. Surface reflection is mostly specular (light is reflected at the same angle of the incident beam). This component is dominant for optically flat surfaces, i.e. having irregularities smaller than the wavelength of the incident radiation [17], while rough surfaces give rise to diffuse reflection (light reflected in all directions). Diffuse reflection is also the major component in volume reflectance because the light coming out from the sample undergoes refraction and reflection prior to its detection. Additionally, when dealing with external reflection from an optically dense sample, the complex refraction index is only in part connected to the absorption index, i.e. to the composition of the analysed spot/layer, as another contribution arises from the variation of the speed of light moving from one medium (air) to another (the sample). Both the parameters are not constant but variable in the infrared spectral range of interest and define the reflectance profile. All these contributions occur while working in external reflection, affecting the resulting spectral bands. At the same time, the presence of strongly absorbing compounds (i.e. organic or carbonate/sulphate/phosphate species) results in inverted spectral bands, while most organic molecules are responsible for derivative-shape bands [18]. Several transformations and correction algorithms have been developed [14], none of which constitutes a perfect model for external reflection analysis.

2.2. Staining - state of the art and effects on protein

Over the past 30 years the detection of proteinaceous media in cultural heritage samples has been also attempted using several methods developed from proteomics: colourimetric/reverse stain, as well as fluorescent stain methods [19]. Of the two, fluorescent staining has the advantage of a linear correlation between optical density and concentration [20], higher sensitivity and avoids protein dissolution due to aqueous staining media [21]. In cultural heritage, fluorescent staining is an alternative method to non-fluorescent visible stains such as Rhodamine B, Amido Black, Acid Fuchsine, Ponceau S, Stain-all or Oil Red O, for the detection of organic paint media in cross-sections [22]. However,

both non-fluorescent and fluorescent stain results can show false positives, false negatives and ambiguous outcomes [23]. Within the biological sciences, there are several fluorescent stains used for protein detection, the main class is based on electrophoretic separation or sensitive detection methods by metal ions, colloids or metal chelates [21]. Of these, the metal chelate staining involves a simple and fairly fast procedure at room temperature. Additionally, it is relatively inexpensive since it does not utilize precious metals such as gold or silver. Complexes form at acidic pH and develop when the pH is increased from 7.0 to 9.0. As the metal chelate blot stain is applicable for protein detection in solid-phase supports [24], it appears quite suitable for paint cross-sections.

SYPRO™ Ruby is a permanent luminescent metal chelate stain used as an alternative to traditional stains in its gel or blot stain formulation. To the authors' knowledge, its full composition is not disclosed: Rabilloud and co-workers [25] suggested that SYPRO™ Ruby contains an organic transition metal chelate, ruthenium II tris (bathophenanthroline disulfonate), RuBPS. However, the commercial product is not a simple solution, as the patent, IPN: WO 00/25139, describes several "embodiements" for staining mixtures comprising a metal ion or unstable isotope coordinated with one or more nitrogen donor ligands [26]. This type of metal chelate interacts non-covalently with proteins [24,25]. It does not show fluorescence in solution, but it becomes fluorescent after this selective interaction. Stained proteins are excited by ultraviolet, at 200–400 nm [27], or visible light (full width at half maximum, FWHM, 388–500 nm, peak position at 470 nm, [28]). As specified by the supplier, the fluorescence emission of the dye is in the 593–710 nm range (FWHM) and shows a maximum at 631 nm [29]. Such difference between excitation and emission wavelength allows for an excellent detection with blue light (LED or filtered visible broadband source), even when protein content is in the order of nanograms [21,23,29]. Additionally, it has been suggested [21,23] that the fluorescence in emission is different from any autofluorescence known to occur in paint samples, thus allowing clear distinction of even the thinnest proteinaceous layers.

According to Schäfer [23], SYPRO™ Ruby does not modify proteins, while Rabilloud [25] has shown that the main compound, RuBPS, does not interfere with other protein detection methods, like mass spectrometry. However, the possible changes to the samples, shifts and intensity variations in FTIR bands that may occur after this staining protocol, have yet to be assessed. This is the case in protein samples, or in more complex and multi-layered systems, where IR vibrations can derive from both organic and inorganic components.

The solubility of proteinaceous layers has been highlighted as a potential issue for all protein staining procedures, which causes original materials to be lost (washed out) during pre-treatment, staining and rinsing/cleaning steps. The degree of swelling, leaching or dissolution depends on the type of binding medium and solvent applied [23]. In the case of aqueous solutions, additional factors such as pH, temperature and ionic strength are also important. Furthermore, the exposure time is a determining parameter to control or minimize sample alteration and loss. The swelling of layers is undesirable as the spatial distribution is compromised and adjacent layers may be covered. The surface of the swollen layer may be in one focal plane while other unaffected layers remain in a lower plane. Hence, the area of interest may be greater than the depth of focus of the microscope and difficult to be observed and analysed by most analytical techniques. However, Schäfer [23] has demonstrated that a proper fixation procedure before the application of the staining solution can prevent severe loss of proteinaceous material and hence enhance the quality of the result.

2.3. Design of the experimental research

Based on the published literature and previous staining and FTIR applications, SYPRO™ Ruby tests and IR spectroscopy were used in combination in this research. μ-FTIR analysis was conducted before and after staining on cultural heritage multi-layer samples where the identification and characterization of organic compounds is of importance for understanding the technique used in their creation and assessing degradation. Different preparation methods were compared: cross-sections were embedded in polyester resin or analysed from loose fragments mounted in a synthetic material to allow the analysis of a complex stratigraphy without the interference of the casting medium. External and internal (ATR-FTIR either with diamond or germanium tip) reflection were compared to transmission data in a reference sample of rabbit skin glue, to determine whether amide bands could be used for mapping purposes, despite the complexity of spectral distortions that are known to occur in external reflection, and for this purpose the staining was used as control test. Within these modes, μ-FTIR on a loose fragment or cross-section has been rarely used for mapping purposes [30], despite it represents a non-destructive mode of analysis to characterise materials by either point analysis or mapping. ATR-FTIR is not always a good approach, as the cross-section can shift while the crystal moves on the surface, causing the mapped area to be shifted and the mapping of specific compounds not to correspond to the right layer. For this purpose, a first extensive comparison of protein μ-FTIR vs ATR-FTIR profiles is provided. These spectral profiles are then used to map protein. This protocol avoids complex data treatment using multivariate statistics [30], which requires a high level of experience to give reliable interpretation.

Rabbit skin glue, as a loose fragment and embedded in resin, was preliminarily tested to develop a protocol for the combined use of staining and FTIR analysis, including data processing, for enhanced protein detection. We decided to focus the present research on rabbit skin glue because this is one of the most common materials used for sized canvases. A representative set of case studies was then selected based on ongoing technical art history and conservation research in progress at the Kelvin Centre for Conservation and Cultural Heritage Research, University of Glasgow, UK. Two samples from 'Hector's farewell to Andromache', an easel painting by Gavin Hamilton (1723–1798), The Hunterian (University of Glasgow), and two samples from the historic Paint Room at the Citizens Theatre, Glasgow were also studied (for further details see the Appendix). These samples were chosen for the range of different materials and variety, exemplary for the effect of SYPRO™ Ruby on multi-layered systems and the need to find the best methodology for interpretation.

3. Materials & methods

3.1. Samples and case studies

3.1.1. Rabbit skin glue reference samples

A rabbit skin glue (RSG) sample (record number F072) was made in 1999 by C. Young as part of the Leverhulme research project ('The Biaxial Properties of Paintings on Canvas', F/624/C). The sample was made by mixing 1 part of RSG with 5 parts of water, soaking until the RSG was swollen, heating to dissolve the RSG, and then pouring onto a non-silicone release sprayed glass with a silicone side retainer then left to dry in ambient conditions. It has since been stored in the dark in ambient laboratory conditions. This sample was chosen because it was sourced as a pure rabbit skin glue and has now naturally aged, thus being a good reference for the effect of SYPRO™ Ruby on the protein alone.

Two small fragments of the same RSG reference sample F072, one without staining and one already stained, were additionally embedded in resin to be studied as cross-sections and determine the effects of staining in combination with the contribution of resin in protein detection by μ-FTIR.

Additionally, other reference samples were embedded in resin for comparison: for the size – rabbit skin glue (1:10 RSG:water by weight) on canvas – and for a slightly more complex stratigraphy, sample MO25. MO25 is a lead-based ground on warm-sized (1:20 RSG:water by weight) linen canvas, produced in 1999 within the Leverhulme research project 'The Biaxial Properties of Paintings on Canvas' (F/624/C).

3.1.2. Cross-sections in casting resin of case studies

Samples for cross-sections from a case study as part of the PISTACHIO project (Photonic Imaging Strategies for Technical Art History And Conservation) were taken from the painting 'Hector's farewell to Andromache' (see details in the Appendix). These samples were chosen as optical microscopy had shown an unusual layer structure in the preparation and ground layers. A small fragment of each sample was mounted in Technovit 2000 LC (Heraeus Kulzer, Germany), a one-component methacrylate resin routinely used at the Kelvin Centre because of its fast polymerization under UVa light (315–400 nm). After preliminary grinding with silicone-carbide (SiC) paper, the surface was dry polished with Micro-Mesh® sheets using grades from 1800 to 12000.

Sample S28 comes from Andro's cloak, painted in dark blue. Analysis was carried out on the cross-section (Fig. 1, a and b) before and after staining. Several layers had been previously identified, from top to bottom: v = varnish; p2 = second pigmented layer, blue; p1 = first pigmented layer, dark blue; g = ground; pr = preparatory organic layer; s = a possible thin size with dark particles.

Sample S27 is representative of the flesh tones on the baby's arm. The protocol of S28 was also applied to this cross-section (Fig. 1, c and d), starting from point analysis and then proceeding with μ-FTIR mapping, before and after staining. A complex stratigraphy had been previously described even for S27 (from top to bottom): v = varnish; p4 – p1 several pigment layers, from red to yellow; wg = whitest ground; g = ground; pr = preparatory organic layer; s = thin size with dark particles, yet to be confirmed. For both samples, the specific focus was on the organic layer *pr*.

3.1.3. Loose samples: The paint frame cross-sections

Amongst the samples collected from the Citizens Theatre (see details in the Appendix), samples LHS_C (Fig. 2a) and LHS_D (Fig. 2b) were both taken from the wall on the left-hand side of the paint room and selected for this study.

As a generous amount of sample was available for both, μ-FTIR analysis was attempted without a casting medium. The identification of organic binding media components in the individual layers of these samples can help provide information on the periods from which theatrical cloths painted on the paint frame originate. LHS_C is believed to be representative of seven early layers in the history of the Theatre. It was chosen for the simplicity of its stratigraphy compared with other samples collected from the paint frame, thus allowing clearer observation of the effects of the staining solution. LHS_D has a more complex stratigraphy, which includes more than 20 layers, thus reflecting the variability as paint splattered off the scenic artists' brushes while the cloths were being painted.

A small support was made for the samples from polyethylene foam, and a small cut was made in it to create a pocket that would house the sample. The side of the sample showing the stratigraphy of interest was polished by hand on the finest Micro-Mesh® sheet (12000 grade) by holding the sample with a precision grabber tool. When the stratigraphy appeared flat and homogeneous, the sample was put face-up into the pocket and its positioning was checked under the microscope. Because of the fragile consistency of the samples taken from the Citizens Theatre and the delicate holding system built for it, the analysis was carried out by μ-FTIR imaging only. The observation of the sample under visible and UV fluorescence optical microscopy led to the recognition of several layers (Fig. 2), where different classes of inorganic (sulfates and carbonates, along with silicates and oxalates) and organic compounds were identified by μ-FTIR. Particularly, in those inner layers described as the most porous and thick under optical microscope, the presence of protein was postulated.

A summary of the whole sample-set is given in Table 1.

3.2. Staining

Fluorescent staining was carried out to detect proteinaceous binding media with the metal-chelate blot stain SYPRO™ Ruby. It was selected because it is one method used at the Kelvin Centre for paint cross-sections. The staining protocol developed by Schäfer [23] was applied as described below.

Fixation. The samples were placed on glass slides supported by small Teflon blocks (ca. 2 × 2 cm) in a beaker. A formaldehyde solution (37% formaldehyde solution in H_2O, 10–15% methanol as stabilizer, Fisher BioReagents) was added to cover the bottom of the beaker. After the beaker was sealed with Parafilm to prevent evaporation, the samples were left exposed for 12 h at room temperature. They were then removed and left to dry for 6 h before the application of the stain.

Application. A small drop of SYPRO™ Ruby Protein Blot Stain (Thermo Fisher Scientific) was directly applied on the cross-section using an Eppendorf pipette, avoiding contact between the surface of the cross-section and the tip. The solution formed a drop, which was left on the surface from 1 to 3 minutes, depending on the effectiveness of the positive staining observed under optical microscope. Any excess staining solution was then removed using a lint-free tissue, avoiding contact with the surface of the cross-section. The sample was left in the dark for a further 5 minutes to allow for complete evaporation and drying of the staining solution and favour the full development and photostability of the fluorophore.

3.3. Optical microscopy

Loose fragments and cross-sections were preliminary observed by an Olympus BX41 microscope, equipped with an external 100 W halogen lamp (U-LH100L-3) and a controllable fluorescence illumination System CoolLED pE-300ultra. Images were collected by an Olympus DP74 colour camera controlled by the software Olympus Stream Basic 2.4.4.

After staining, the samples were observed with the same optical microscope equipped with a U-MWB2, UV/yellow filterset: excitation band-pass filter at 460–490 nm; suppression long-pass filter at 520 nm. The distinctive red–orange emission from proteinaceous layers stained by SYPRO™ Ruby was observed and recorded with exposure times from 700 ms to 1 s.

3.4. FTIR spectroscopy

Spectroscopy analysis was conducted using a Thermo Scientific™ Nicolet™ iN™10 Infrared Microscope equipped with a mercury cadmium telluride (MCT) detector, which allowed the acquisition in the spectral range 4000–675 cm^{-1}.

For the RSG reference sample, different configurations were tested: ATR-FTIR using either a germanium slide-on (ATR_iN10) or diamond (ATR_iZ10) micro-tip crystal, and μ-FTIR (iN10 microscope) in transmission and external reflection. The parameters for the analysis were kept constant for each configuration: 64 scans and 4 cm^{-1} resolution. The microscope aperture was set at 50x50 μm. The selected apodization was Norton-Beer strong.

For the Citizens Theatre samples mounted in polyethylene foam, a representative point on each layer identified by optical microscopy was analysed in reflection mode (8 spots, 64 scans, 8 cm^{-1} resolution) to obtain explorative spectra, closely examined and compared for the assignment of typical bands to a range of possible components. This was followed by an area analysis across the stratigraphy of the sample, which allowed the mapping of possible components in specific layers.

To describe the effects of staining on cross-sections in resin, the parameters selected for point analysis were: 16 sample/background scans, 5-second sampling intervals, 4 cm^{-1} resolution and Norton-Beer strong apodization. Maps were collected with the following parameters: 64 sample/background scans; 12-second sampling intervals; 8 cm^{-1} resolution and Norton-Beer strong apodization; variable step-size, depending on the stratigraphy of the sample (height in the range 10–15 μm; width 10–25 μm), and aperture size of 100x100 μm.

Data were analysed using the software OMNIC™ Picta (Thermo

Fig. 1. The painting 'Hector's farewell to Andromache' by Gavin Hamilton (Acc. nr. GLAHA:44127), from the Hunterian Art Gallery, University of Glasgow, with the sampling points for the samples studied in the paper (top); OM pictures (scalebar = 100 μm) of the cross-sections, under visible and UV light: S28, (a-b, stacked) and S27 (c, normal, and d, stacked).

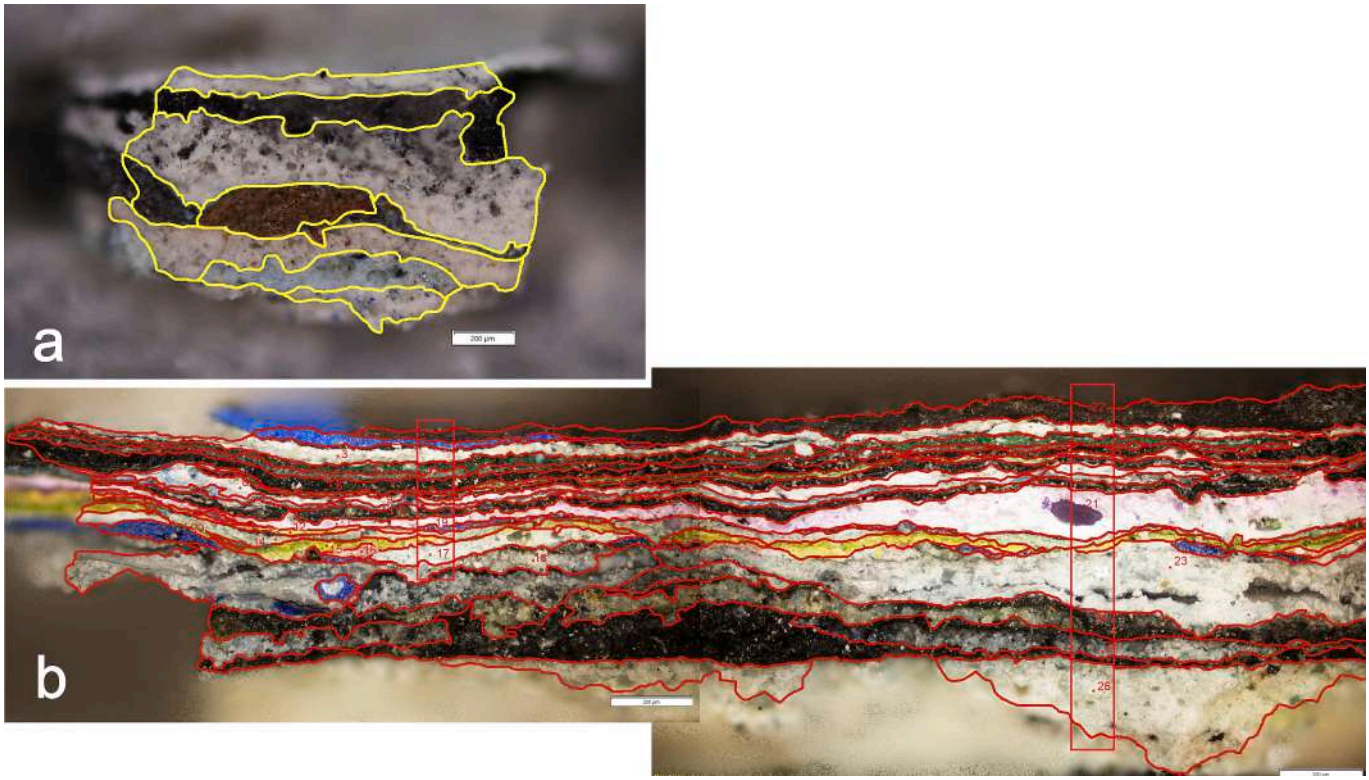

Fig. 2. LHS_C (a) and LHS_D (b) samples from the left-hand side of the paint room in the Citizens Theatre in Glasgow, observed under visible light by OM, with layers and μ-FTIR analysis outlined (red dots = point analysis, rectangle = imaged area; scale bar = 200 μm).

Table 1
Summary of all the samples (mock-up and case studies) mentioned in the paper and analysed by μ-FTIR before and after staining. F072 was additionally analysed with ATR and transmission mode FTIR.

	Sample	Description
MOCK-UP SAMPLES	F072, loose	Rabbit skin glue, uncast, unstained
	F072, cross-section	Rabbit skin glue embedded in resin
	F072, stained, cross-section	Rabbit skin glue embedded in resin after staining
	Size, cross-section	Rabbit skin glue on canvas embedded in resin
	MO25, cross-section	Lead-based ground on sized canvas embedded in resin
CASE STUDIES	S28, cross-section	Sample from Andro's cloak, painting "Hector's farewell to Andromache", by G. Hamilton, embedded in resin
	S27, cross-section	Sample from the baby's arm, painting "Hector's farewell to Andromache", by G. Hamilton, embedded in resin
	LHS_C, loose section	Sample from the left-hand side wall of the Citizens paint frame, hold in polyethylene foam
	LHS_D, loose section	Sample from the left-hand side wall of the Citizens paint frame, hold in polyethylene foam

Fisher Scientific). Spectra from point analysis were compared in the fingerprint region. Corrections such as baseline subtraction, Kubelka-Munk or Kramers-Kronig were applied when needed as specified in the results section. False-colour maps were built on either single peak height/area or two peak height/area ratios. Correlation maps with reference spectra were also considered to visualise the distribution of protein in cross-sections, especially to separate it from the contribution of the embedding resin.

4. Results and discussion

4.1. Reflection infrared and staining properties of rabbit skin glue

A positive staining was observed for all RSG samples (Fig. 3), loose or embedded in resin, even five months after the treatment.

FTIR data were analysed for comparison between the different acquisition modes described in 3.4 and at each stage of the staining protocol: before treatment, after fixation and after staining (see Table S1).

Collagen is the structural protein of rabbit skin, which is known to contain an aminoacidic sequence where glycine, proline and hydroxyproline repeat and are held together by strong oxygen bonds. These bonds are broken and replaced by bonds to water in gelatine, which derives from the processing steps of rabbit skin to produce a glue [19]. The spectra of RSG acquired before staining showed the characteristic vibrations of amides in the 1700–1200 cm^{-1} range, i.e. the functional group in amino acids containing a carbonyl group and nitrogen atom and interacting with IR radiation [31]. The most intense band is the amide I, due to carbonyl stretching vibrations, while the amide II is primarily given by N–H bending vibrations [32]. The third most intense band, the amide III, represents the in-phase combination of the N–H bending and the C-N stretching vibrations [33]. In the spectra collected for this study, several changes occurred in the main amide bands depending on data treatment or preparation of the sample, as described below.

a) Data treatment

ATR-FTIR data acquired with diamond or germanium tip only shows a difference in the intensity of the main amide bands, which can also depend on a different degree of contact between crystal and sample. Important shifts in band position were seen between spectra collected in external reflection (Fig. 4a – I) and transmission/ATR (Fig. 4a - III) and

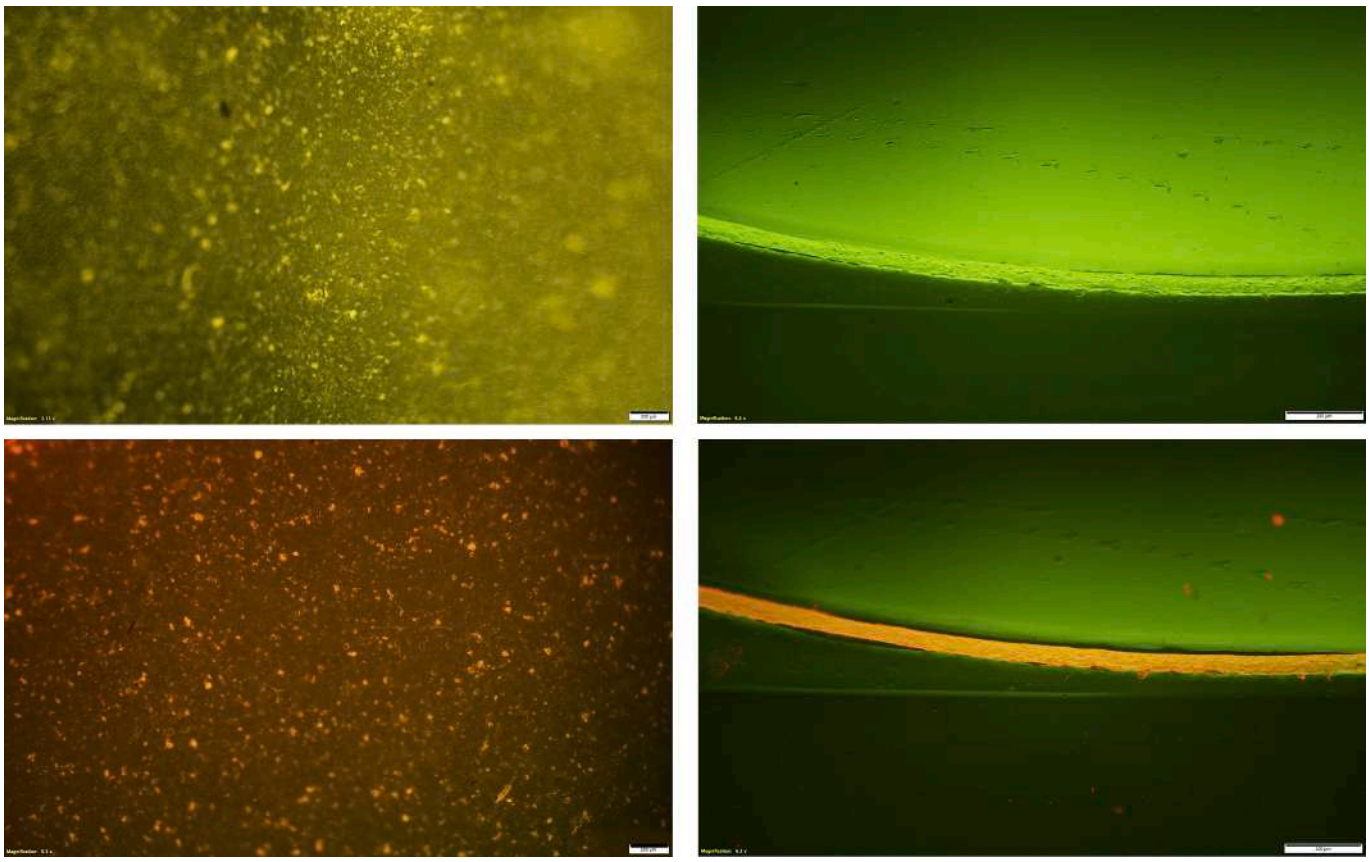

Fig. 3. Rabbit skin glue before (top) and after (bottom) staining, loose (left) or embedded in resin (right) under blue excitation (U-MWB2, UV/yellow filterset; scalebar: 200 μm).

can be explained by the different contributions of specular and diffuse reflectance [14,34]. In the fingerprint region, transmission and ATR data have good agreement, amide I and III bands being respectively at ~ 1630 and 1453 cm^{-1}, while the amide II varies from 1531 (transmission) to 1548 (ATR) cm^{-1}. In external reflection, the amide I band is intense and narrow, the highest intensity being at 1694 cm^{-1} and 1685 cm^{-1} in the loose and embedded RSG respectively. Amide II and III bands are markably lower in intensity, the highest value being recorded at 1574 and 1471 cm^{-1}, respectively, in the loose RSG. The inflection points for these bands, calculated by first derivative and Savitzky–Golay filter (21 points, 2nd order) at 1672 and 1558 cm^{-1}, are higher than the band maxima obtained in transmission/ATR (Table S1), while their minima (1628 and 1537 cm^{-1}) are lower. This result demonstrates that when rabbit skin glue is not embedded, protein signals tend to have intermediate features between derivative-like and inverted bands. Embedded RSG showed similar behaviour, the inflection points being at 1666 and 1549 cm^{-1} and band minima at 1629 and 1521 cm^{-1}. In the 3800–3200 cm^{-1} region, the amide II overtone has its maximum at higher wavenumber in the raw spectrum of the loose RSG (3103 cm^{-1}), than when embedded in resin (3087 cm^{-1}). In both ATR and transmission mode, the band maximum is at ~ 3076 cm^{-1}, showing that even this band is affected by slight changes when the sample is analysed in external reflection.

Kubelka-Munk (K-M) correction is the approximate model that can be applied to describe the behaviour of diffuse reflected light, after its interaction with polished cross-sections or optically flat samples which show strong IR bands in the fingerprint region, as the main amide bands of protein. However, when the K-M correction is applied, band position and shape do not change with respect to raw spectra, demonstrating that it is not efficient to represent the interaction with IR light in this type of sample. Reflected light has mainly a surface component that could in principle be corrected by the Kramers-Kronig (K-K). However, in the published literature on external reflection corrections to cross-section experiments [15,30] it has been postulated that the K-K transform cannot be applied as the IR light reflected from this type of samples contains both surface and volume reflection. Since both K-M and K-K models constitute a partial correction in non-ideal samples and may lead to erroneous interpretations, it was decided to mainly focus on raw μ-FTIR spectra for all the other samples. The identification of proteins is in fact possible without any of the aforementioned processing if one considers the mixed derivative-like or inverted appearance of protein bands in external reflection mode, due to the combination of surface and volume reflection [14,30]. The following experiments are aimed at describing spectral features for different types of samples, before and after staining, in order to find the best mapping strategy for cultural heritage objects.

b) Type of sample and staining step

When μ-FTIR spectra collected before and after staining are compared, several vibrations are consistently present at any stage of the staining, but they are affected by small shifts in peak position. In the loose fragment (Fig. 4b - I), after staining (as) the amide I band is affected by a positive shift (from 1694 to 1701 cm^{-1}), while amide II and III undergo a slightly negative shift, respectively from 1574 to 1570 cm^{-1} and from 1472 to 1466 cm^{-1}. Intensity ratios of amide II/amide I and amide III/amide I slightly increase (+0.01) after staining, possibly suggesting a decrease in derivative-like features, i.e. in the impact of the specular component, which we interpret as a negligible change of surface properties.

When the sample is analysed as a cross-section after embedding (Fig. 4b - II), resin bands, especially the most intense one at 1748 cm^{-1},

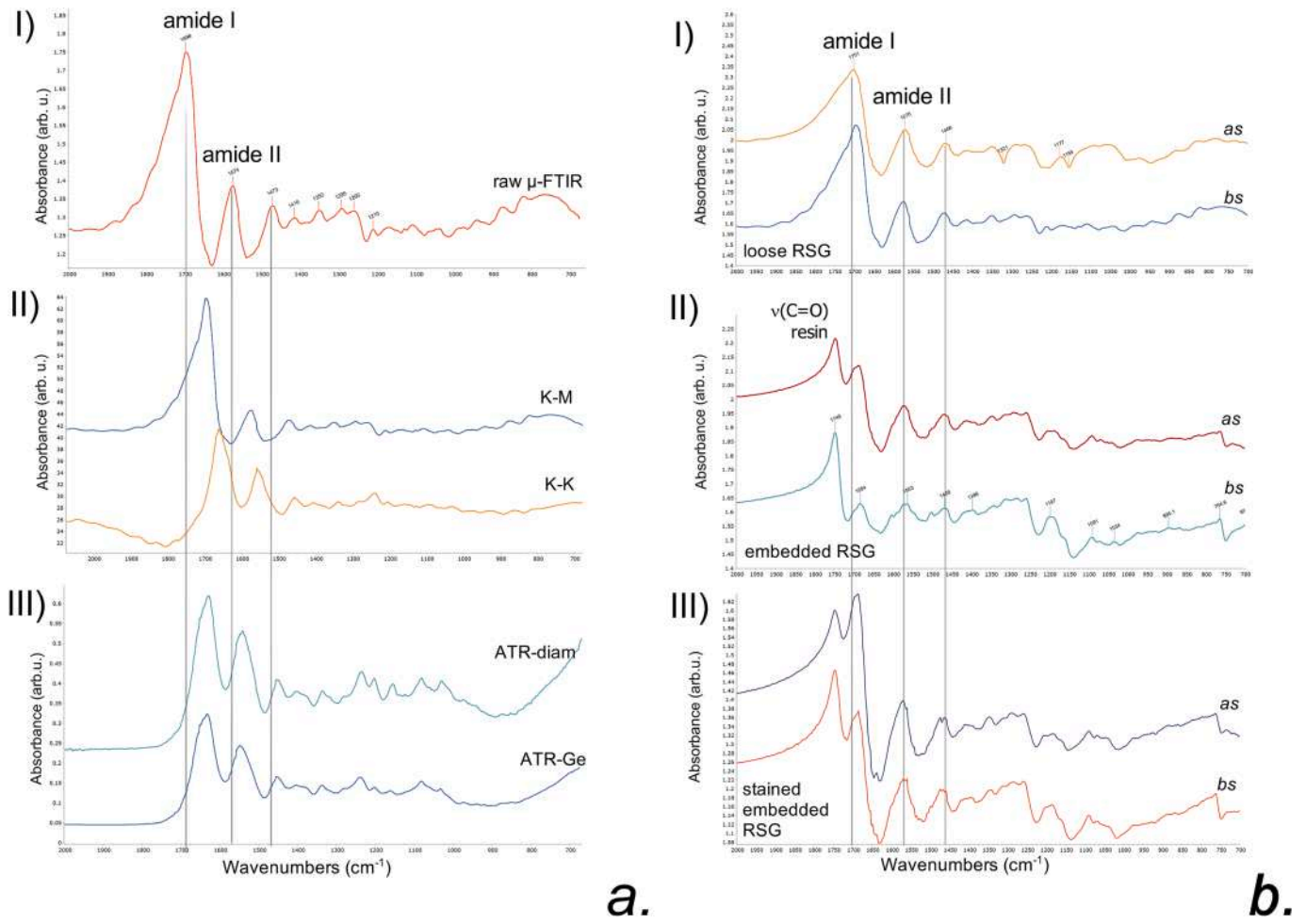

Fig. 4. a) I. raw μ-FTIR spectrum of the loose fragment of RSG, with main protein bands, compared to the spectra given by different data processing, II (K-M or K-K correction) or different collection mode, III (ATR with germanium, ATR-Ge, or diamond, ATR-diam, tip); b) I. raw μ-FTIR spectrum of the loose fragment of RSG, with main protein bands, collected before (bs) and after (as) staining; comparison with the raw μ-FTIR spectra of the embedded RSG (II) and of the stained embedded RSG (III).

interfere with protein bands. Amide I and II respectively shift from 1694 and 1574 cm^{-1} in the loose RSG, to 1685 and 1560 cm^{-1} in the embedded sample. Additionally, the contribution from bands at lower wavenumbers can hardly be detected. The highest positive shift in position is recorded for amide II after staining (+11). In the embedded RSG, intensity ratios (amide II/amide I and amide III/amide I) decrease with respect to the loose RSG (-0.05), meaning that the derivative-like feature of amide bands increases after staining, possibly as a result of swelling mechanisms.

The RSG stained fragment was also embedded in resin and stained again (Fig. 4b - III). The position of the main bands was not affected by the second staining. However, the amide I band intensity was higher than that of the main resin band. This suggests that, in the case of low concentrations or very thin layers, a double staining can increase the detectability of protein in cast samples. However, this result might also imply an increased derivative-shape behaviour of the amide bands, possibly linked with higher variation of surface properties due to a more pronounced swelling, as demonstrated by the further decrease of intensity ratios (-0.13). As additional proof of swelling, the average thickness measured on visible light OM images before the staining (44.5 ± 1.8 μm) was found to be lower than after it (51.0 ± 1.8 μm). The latter has good match with the value calculated on images taken with the U-MWB2 filter (48.8 ± 2.4 μm). The higher standard deviation is a result of the difficulty in assessing the thickness from a fluorescent layer.

μ-FTIR mapping of the embedded RSG samples after staining was useful to define the methodology for effective visualisation of thick proteinaceous layers in a casting medium. Due to the difficulty in determining band maxima because of spectral distortions, peak-height mapping was not considered and two false-colour maps (S2, a-b) were made based on peak area (spectral range at 1716–1678 and 1630–1520 cm^{-1}, for amide I and II respectively). These maps have good agreement with protein distribution and thickness based on staining results.

Alternatively, false-colour maps built on two peak-area ratios could be used to represent the proteinaceous layer in good agreement with the positive staining. The ratios were calculated based on the two most intense protein bands and the main resin band area (Fig. S2c for amide I, and Fig. S2d for amide II). All maps gave a layer thickness varying between 50 and 53 μm, in good agreement with the OM measurements.

The latter data treatment led to an overestimation of the thickness in the double-stained RSG cross-section, possibly because of the inverted intensities of the amide I/resin (Fig. S3a) or amide II/resin (Fig. S3b) band ratio. The false-colour map built on the peak area of the amide II band (integration between 1630 and 1530 cm^{-1}, Fig. S3d) gave the best approximation of thickness (67–70 μm), despite in slight disagreement with the average value from optical microscopy measurement (59.2 ± 2.6 μm). The amide I band area (integration range 1722–1677 cm^{-1}, Fig. S3c) showed lower thickness (51–54 μm). For this sample, all the false-colour maps reported a displacement of the layer when compared to microscopy pictures, possibly depending on instrumental parameters, such as acquisition step or resolution.

4.2. Reflection infrared and staining properties of mock-up samples

In both types of mock-up samples, the isolation of protein bands in μ-FTIR spectra was particularly challenging, possibly because of the low glue content within the linen fibres of the canvas. In the size, the position of protein signals was found not to change before and after staining: the main amide I band was recorded at 1685 cm^{-1} before staining and at 1688 cm^{-1} after it; amide II and III did not change in position (at 1565 and 1467 cm^{-1} respectively), but were found to have lower intensity after staining (Fig. 5a). These results prove that, despite this sample having different surface properties when compared to pure RSG, the spectral behaviour of the protein does not change when embedded in resin. Fig. 5b shows a possible increase in protein detection after staining, when false-colour maps based on the amide I peak height are compared. After the staining, the increase of the resin band at 1603 cm^{-1} and 1506 cm^{-1} was observed, possibly confirming the swelling of the glue inferred from OM observations.

In a more complex stratigraphy, as in the case of the cross-section including a ground (MO25), it was not possible to detect protein bands before the staining. After staining, the amide I band was identified at 1674 cm^{-1}. However, the false-colour map based on this peak height did not match with the staining, showing that the size is only distributed in small interstices between two yarns, below the ground (red dotted contour in Fig. 6a). As in this sample a warm size had been applied, penetrating the linen yarns and into the fibres, the distribution of cellulose in the analysed area cannot be separated from that of collagen. Despite this and the interference from the embedding resin, the staining prior to μ-FTIR analysis aided the visual detection of the protein and a correlation map (false-colours in Fig. 6a) could be obtained using a raw spectrum from point analysis, collected where the orange fluorescence due to staining was the most intense (red spectrum in Fig. 6b). This map seems not to be affected by the contribution of embedding resin or linen

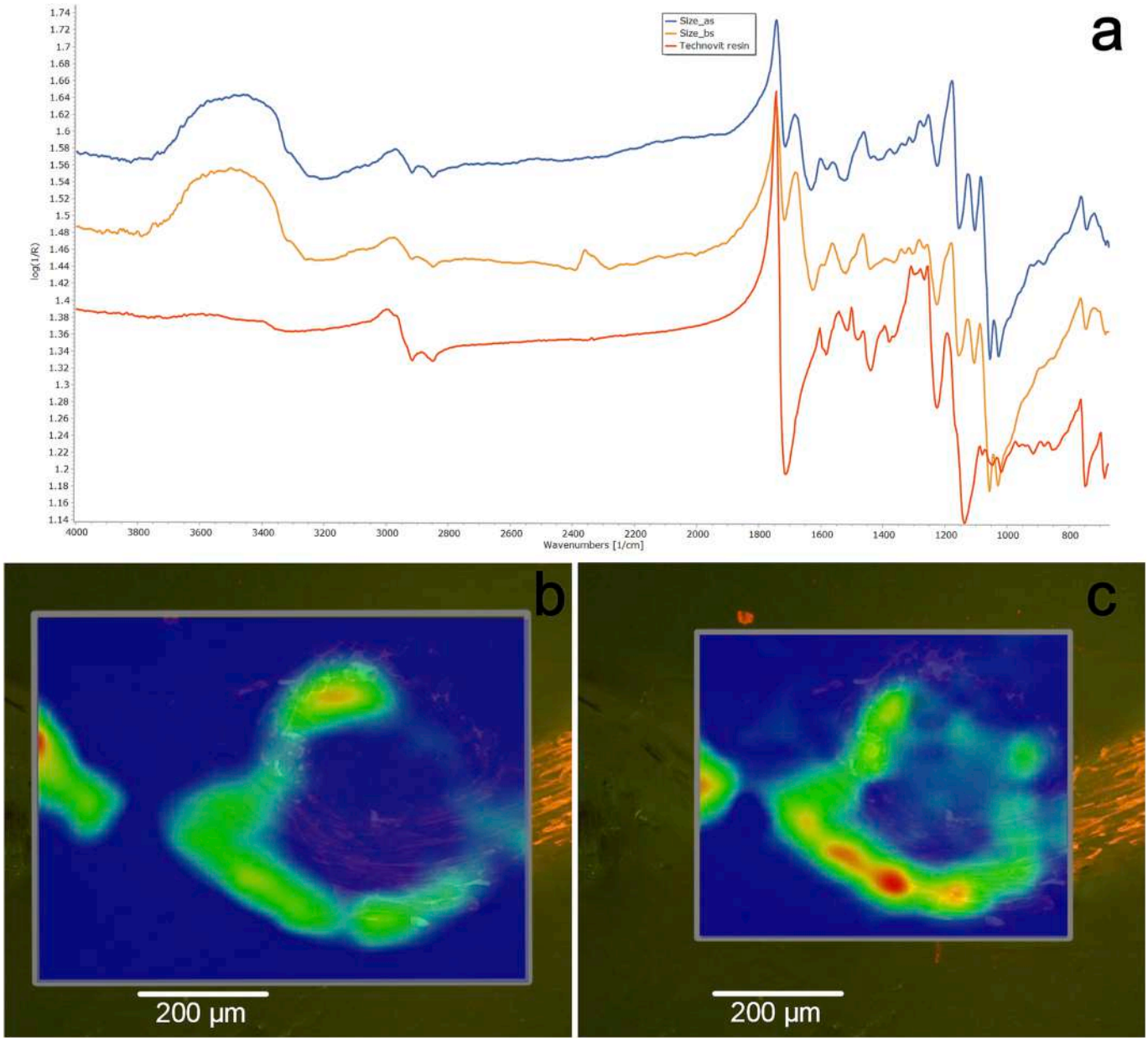

Fig. 5. a) comparison of spectra from the size before (yellow) and after staining (blue), and the one of the Technovit resin (red); OM pictures (U-MWB2, UV/yellow filterset, scalebar = 200 μm) of the size in cross-section where false-colour maps based on the ~ 1683 cm^{-1} peak height before (b) and after (c) staining (integration in the range 1718–1650 cm^{-1}); colour scalebar: red = highest intensity, green = mid-intensity, blue = lowest intensity.

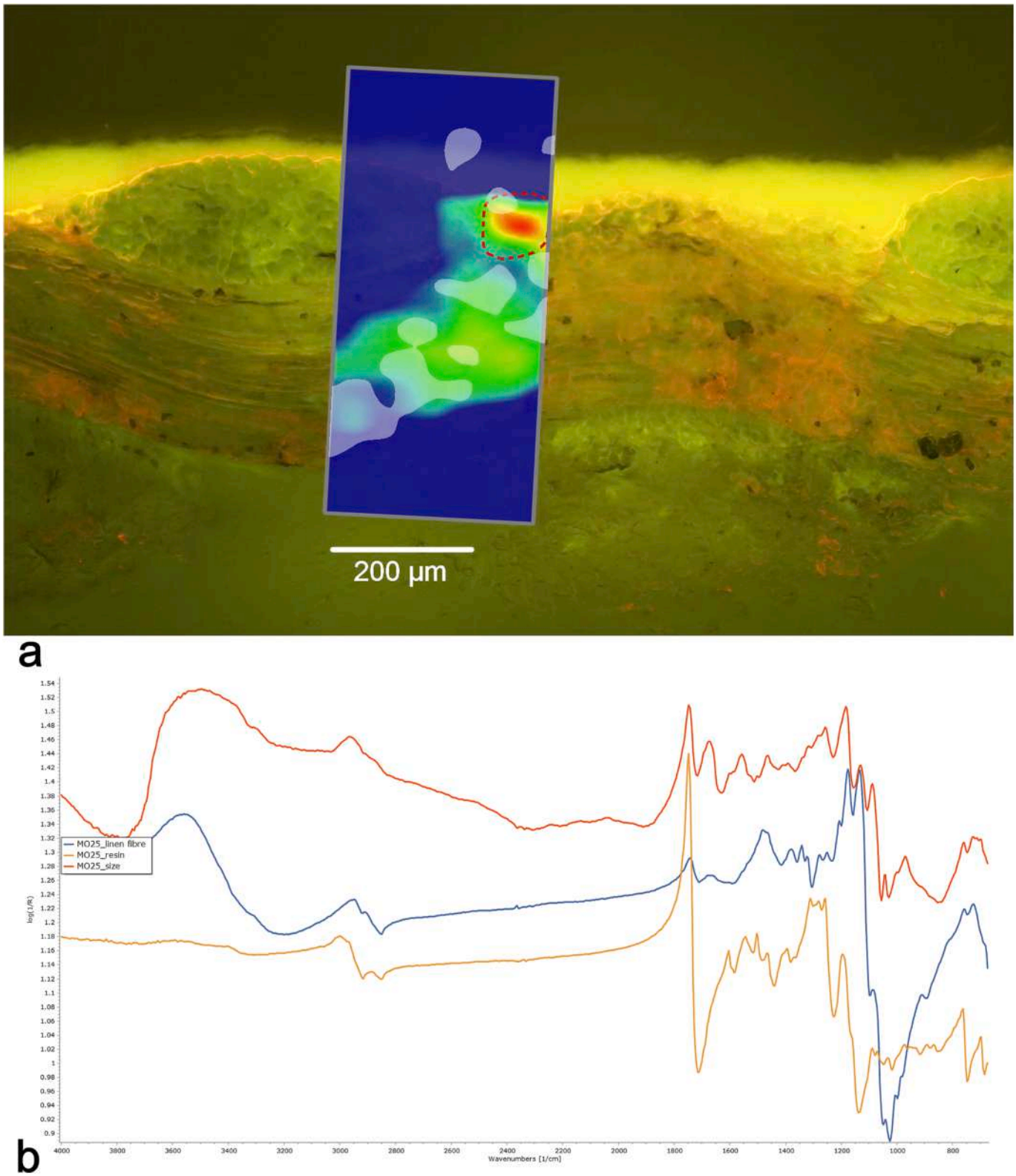

Fig. 6. a) µ-FTIR mapping of protein in MO25 after staining, based on 1674 cm^{-1} peak area (red dotted line), on the 3070 cm^{-1} peak height (white areas) and false-colour correlation map based on the raw spectrum from a point where protein signals were the most intense (colour scalebar: red = highest intensity, green = mid-intensity, blue = lowest intensity); b) comparison between the spectrum of the size used for the correlation map (red), one from the nearby linen fibre (blue) and one from the embedding resin (yellow).

fibres, and is in good agreement with the positive staining. Conversely, the map built by integrating the 3070 cm^{-1} band partially agreed with the staining (white areas in Fig. 6a) and erroneously gave evidence of protein presence above the ground.

It has been postulated that the thinnest layers of positive staining can be false-positive results, as a consequence of the diffusion of the stained protein between canvas and ground [19]. However, in our case the very thin orange-fluorescent layer right below the ground (see Fig. 6a) is likely to be a positive result, because the rabbit skin glue will have diffused through the canvas when warm sized.

The results obtained from the mock-up samples constituted the basis for treating and analysing samples from case studies and describing the presence of protein at best.

4.3. 'Hector's farewell to Andromaque' by G. Hamilton

The staining gave a positive result in the whole organic-based layer (pr) of S28 and S27 and favoured the identification of the amide I band. The comparison of point analysis on *pr* before and after staining showed several variations in spectral features (Table 2).

For example, after the interaction of S28 with SYPRO™ Ruby the band at 1681 cm^{-1} is lower in intensity and it shifts to lower wavenumbers (1675–1666 cm^{-1}) while the amide II band is almost constant (1562—1567 cm^{-1}, Fig. S4). The latter is affected by the interference from the resin band at ~ 1604 cm^{-1}, which becomes more intense after staining, as in the mock-up samples, but also by the strong *reststrahlen* band attributed to the carbonate group, due to lead white (basic lead carbonate) from the ground. Therefore, only the amide I band can be considered for mapping purposes. Despite the higher complexity of these stratigraphies with respect to the mock-ups, spectral features of the protein-based layer seem comparable to MO25 (Table 2). Even if the spectrum from a point with high positive staining is unaffected by the strong interference of the carbonate *reststrahlen* band in the above ground (see Fig. S4), the correlation map built from it shows a protein layer with half the thickness of the positive staining (Fig. 7b). Better agreement with the staining is given by the false-colour map based on peak area after staining (integration in the range 1710—1630 cm^{-1}), despite the morphology of the size is better represented in S28 (Fig. 7c) than in S27 (Fig. 7f).

If a polished cross-section has a flat surface, we might expect the specular component to be predominant and the K-K algorithm to be effective in the correction of derivative-like bands related to organic materials [35]. However, for the cross-sections coming from Hamilton's painting it was found that the K-M correction provides better evidence of protein distribution than the raw spectral features, both in terms of morphology and thickness (Fig. 7d for S28 and 7 g for S27). This was interpreted as the result of swelling due to the staining, which occurred in the mock-up samples, this gives rise to more surface irregularities and hence favours the predominance of the diffuse component over the specular one. Neither the position of the amide I band nor its relative intensity changed when the K-M was applied (Fig. S4 and S5).

4.4. The Citizens Theatre paint frame

When the staining was carried out on loose cross-sections (Fig. 8a), the positive result was found to fade even after 30 min and was almost completely lost after 2 days (Fig. 8b) because of the diffusion of the staining solution through this highly porous sample. μ-FTIR was tentatively carried out straight after the staining, but it was not possible to obtain spectral data with high quality, because the surface was not completely dry. μ-FTIR data of the stained samples were successfully collected after 2 days.

In both the Citizens Theatre samples, most of the peaks assigned to protein in the fingerprint region are in the same position as the strong peaks for sulphates and carbonates [31] and are hard to resolve. However, the chemical composition and the morphology generated by the inorganic component favour the collection of volume reflected light observable by the evident increase of the carbonate and sulphate combination bands. This is also reflected in the amide band positions and shapes becoming similar to positive peaks, which were considered and allowed the identification of protein in layers 4, 6 and possibly 7 of LHS_C and in layer 26 of LHS_D (see Fig. 1), also confirmed by the absence of a lipidic binder, as the carbonyl stretching at 1740 cm^{-1} was not observed [36]. In these samples, the main amide I band undergoes a positive shift after staining (Table 3). At the same time, the most intense *reststrahlen* band (minimum at ~ 1420 cm^{-1}) of carbonate species makes the detection of amide II band difficult, and the latter is most often recorded as a shoulder, only after staining. For sample LHS_D, possibly due to the presence of sulphates, which are characterised by OH units vibrations in the same range, the amide I band is at the highest wavenumbers (1692 cm^{-1}).

Because the amide I band (Fig. 9e) falls in the range assigned to the vibrational modes of several compounds (organic, i.e. carbonyl vibration, and inorganic, i.e. hydration units of sulphates, carbonates and oxalates), amide II was finally chosen to build a false-colour map based on peak area integration (Fig. 9f) and to isolate protein contribution in layers 4, 6 and 7 (Fig. 9c) from those of other species (Fig. 9b).

Fig. 9a and 9d compare the OM images acquired before and after staining, respectively. In this sample, only a weak orange fluorescence was recorded after the staining and before its rapid fading, and it was difficult to match it with μ-FTIR maps.

Despite the positive staining of sample LHS_D being more evident, the amide II peak area map could only be obtained after staining. This is possibly because a side-effect of staining is the partial dissolution of the carbonate fraction with the consequent loss of intensity of the strong carbonate *reststrahlen* band (indicated by the bubbling observed during the staining).

Similarly to LHS_C, the analysis of LHS_D confirmed that the best agreement between μ-FTIR imaging and positive staining is given by the peak area map of the amide II band (Fig. 8c - I), because the amide I band map showed the presence of protein even in layers where the staining was negative, whether it was performed after staining (Fig. 8c - II) or fixation (Fig. 8c - III).

4.5. Guidelines for protein analysis in cultural heritage

The study of different types of samples where proteinaceous layers are present demonstrated that, although different spectral distortions occur depending on sample properties, the main amide signals in external reflection μ-FTIR spectra can be used for protein mapping in simple or more complex stratigrafies. This type of analysis, fast and non-invasive on a micro-sample, or non-destructive on small objects that can be hosted by the microscope stage, avoids the drawbacks of ATR-FTIR, such as sample displacement or damage. The combination of staining and μ-FTIR has been proved to be highly effective in documenting the distribution of what is known/historically likely to be glue in several types of samples. This methodology also led to the introduction of criteria for its easier detection, representation and best data processing for external reflection results. The type of processing strongly depends on the type of sample under investigation. Where the stratigraphy is simple, and thick proteinaceous layers are to be detected, it is sufficient

Table 2
Summary of changes in the position of amide I and II bands in all the samples embedded in resin before (bs) and after (as) staining; nd = not detected.

	AMIDE I (cm^{-1})			**AMIDE II** (cm^{-1})		
	bs	**as**	shift	**bs**	**as**	shift
RSG	1680	1686	+6	1566	1569	+3
Size	1682	1687	+5	1565	1565	=
MO25	nd	1674	–	nd	1557	–
S28	1681	1666	−15	1562	1567	+5
S27	nd	1676	–	nd	nd	–

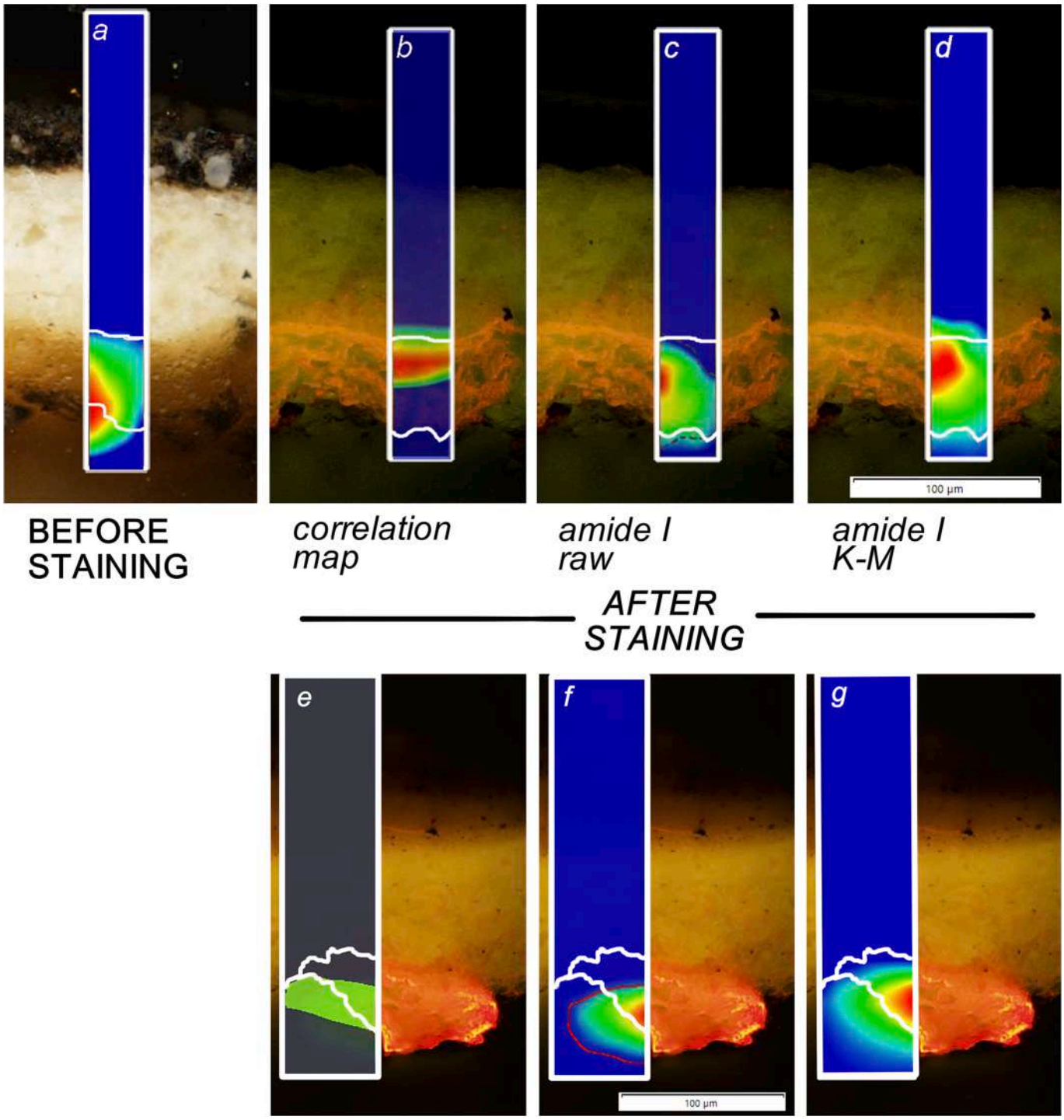

Fig. 7. OM pictures of the cross-sections from Gavin Hamilton's painting (scalebar = 100 µm) to compare staining (white lines) and µ-FTIR mapping results in S28 (a-d) and S27 (e-g): a) under visible light with superimposed 1680 cm^{-1} peak area map before staining; after staining in visible light and U-MWB2, UV/yellow filterset, with b) correlation map from the most intense positive staining; single-peak map of amide I band at ~ 1675 cm^{-1} c) without correction (peak area = dotted line, peak height = false-colour map) and d) with K-M correction; e) correlation map (in green) from the most intense positive staining; single-peak map of the amide I band at ~ 1675 cm^{-1} f) without correction (peak area = red line, peak height = false-colour map) and g) with K-M correction; colour scalebar: red = highest intensity, green = mid-intensity, blue = lowest intensity.

to build false-colour maps integrating the area of the most intense amide I or II bands. The analysis of the rabbit skin glue showed that these bands occur at higher wavenumbers in µ-FTIR (at ~ 1690 and ~1570 cm^{-1} respectively) than in ATR-FTIR or transmission mode, and have intermediate features between derivative-like and inverted bands. Nevertheless, their integration can be used to represent the selected layer with good approximation in shape and thickness.

The analysis of the double-stained RSG sample additionally suggests that the double staining can increase the detectability of protein and the subsequent mapping by µ-FTIR, especially in layers where the amount of protein is low. However, it should be considered that it might also imply an increased derivative-shape behaviour of the amide bands.

On the loose RSG, the position of the main amide bands does not change after staining, proving that they can be considered for quick

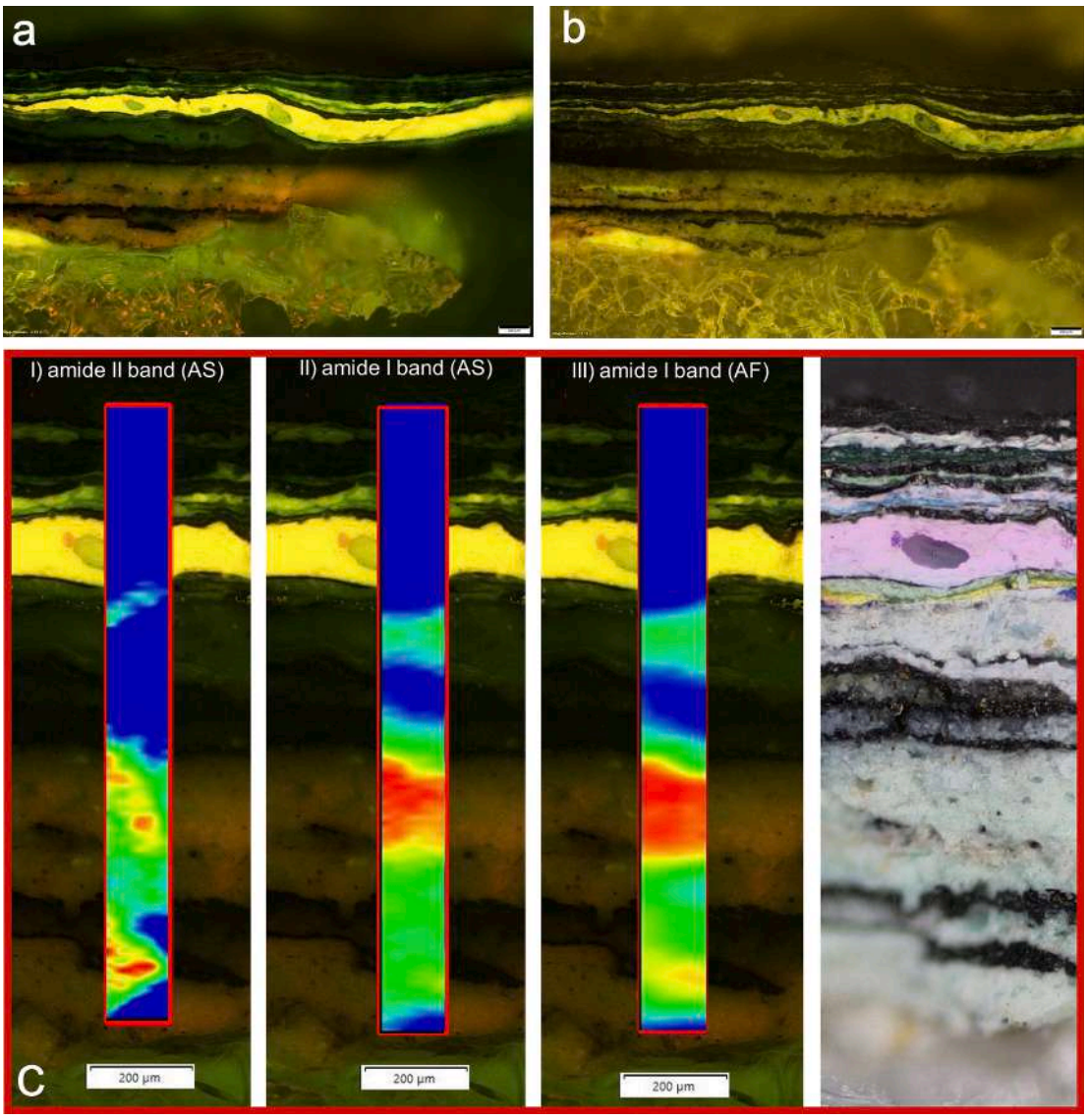

Fig. 8. OM pictures (U-MWB2, UV/yellow filterset, scalebar = 200 µm) of LHS_D mounted in polyethylene foam: after 3 min from the application of SYPRO™ Ruby Blot stain (a) and after 2 days (b); staining result and false-colour maps of I) amide II peak area (calculated between 1620 and 1510 cm^{-1}) after staining (AS); II) amide I peak area (1730–1630 cm^{-1}) after staining and III) after fixation (AF); colour scalebar: red = highest intensity, green = mid-intensity, blue = lowest intensity.

Table 3
Summary of changes in protein band position in the Citizens samples LHS_C (layer 4, Fig. 1a) and LHS_D (layer 26, Fig. 1b), before (bs) and after (as) staining; sh = shoulder, nd = not detected.

	LHS_C bs	LHS_C as	LHS_D bs	LHS_D as
Amide I (cm^{-1})	1664	1677	1662	1692
Amide II (cm^{-1})	1562	1577 (sh)	nd	1577 (sh)
Amide III (cm^{-1})	1452	1450	1461	1455

false-colour mapping, regardless of when the staining is performed. However, this is probably the less frequent situation in cultural heritage samples.

It is usually more common to study protein layers within a more complex stratigraphy, where inorganic and organic compounds occur together, as in grounds where chalk, gypsum or extenders are used with glue. If that is the case, inorganic compounds influence the typical µ-FTIR signals of protein, as they are known to induce *reststrahlen* effects [14]. However, the analysis of the mock-up samples in resin demonstrated that the combination of inorganic and organic compounds, although challenging, does not impede the isolation of IR bands for protein mapping. This can be done by a relatively simple data processing, which considers the peak area ratio of the amide II band of protein and the one of resin to build a false-colour map representing the selected layer with good approximation in shape and thickness, as the comparison with the positive staining showed.

If the size is in a separate layer of the stratigraphy and thick enough to allow the analysis of several data points from it, within the whole area analysed by µ-FTIR, protein bands are well-resolved and can be used to build false-colour maps based on the integration of the amide I or II band. Of these, the amide I is usually more effective, in terms of morphology and thickness of the layer, to describe the presence of protein.

In other samples, glue might have been absorbed by textile fibres, and hence it does not constitute an independent layer, as for the size without/with ground analysed in this study. This being the case, the staining can help to localise the best point to extract a raw spectrum with the most intense protein signals, i.e. where the orange fluorescent

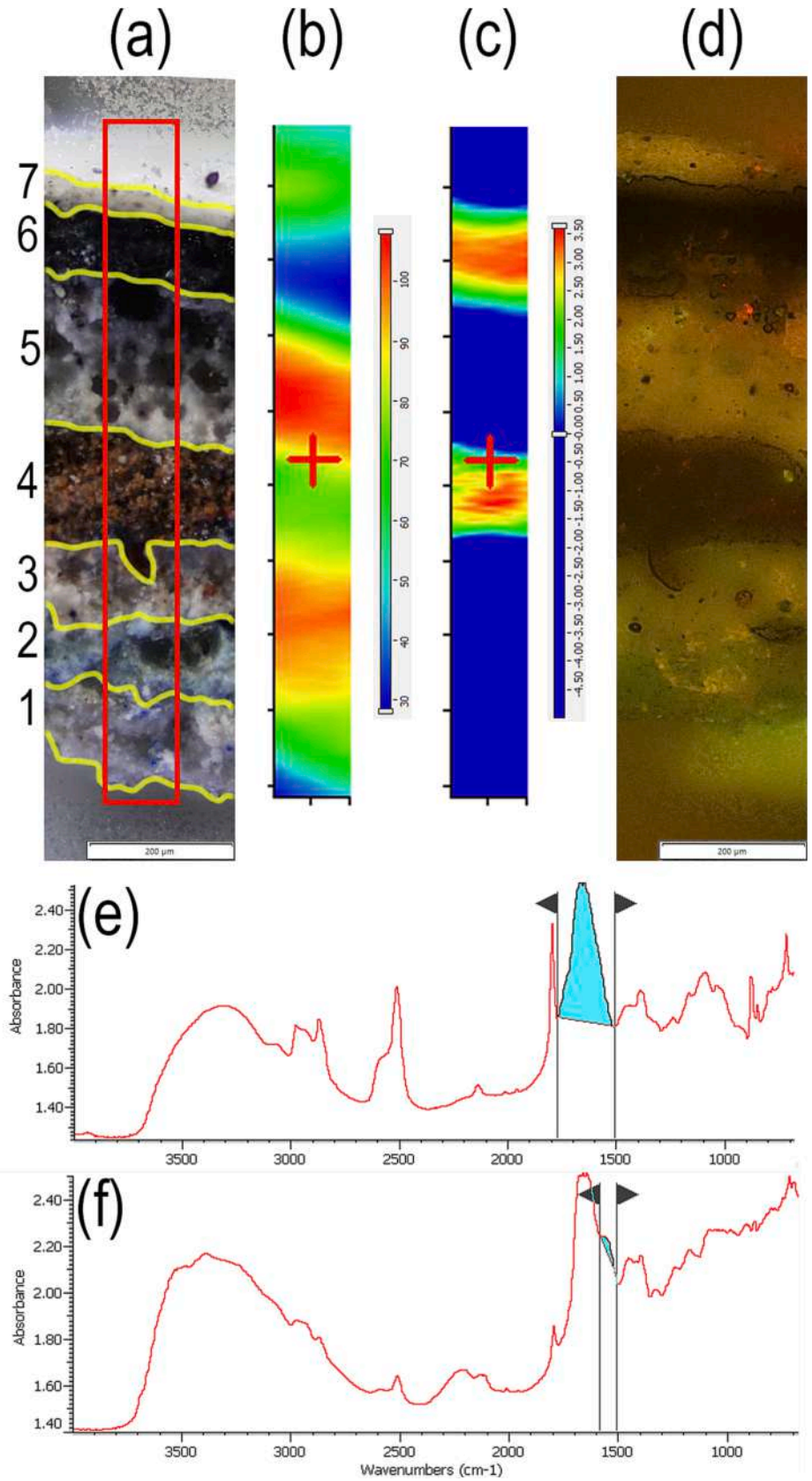

Fig. 9. OM picture (visible light, scalebar = 200 µm) of sample LHS_C with identified layers (a); µ-FTIR maps before staining, extrapolated from the band at about 1680 cm^{-1} (b = result; e = processing) and from the shoulder at about 1550 cm^{-1} (c = result, f = processing); OM picture (visible light, U-MWB2, UV/yellow filterset, scalebar = 200 µm) collected soon after the application of SYPRO™ Ruby Blot stain, with very weak positive result (d).

staining is the highest. This raw spectrum can be then used to build a correlation map with an excellent representation of protein distribution in the cross-section, overcoming the interference from the embedding resin. Even if the staining might enhance the detection of amide bands in raw spectral data, it might cause swelling and the subsequent variation of surface and spectral properties of organic species. As a consequence, the K-M correction can sometimes provide the best approximation of protein layers by the integration of the amide I band area, as it was shown for the Hamilton's painting samples.

Finally, on loose cross-sections, as in the case of the Citizens Theatre, the staining result must be recorded straight after the positive result appears, within 30 minutes from the application, because it rapidly fades, especially in the most porous samples. However, μ-FTIR analysis cannot be performed within the same interval because of the wet surface. For the spectral identification of protein in a loose cross-section, the absence of resin is an advantage but at the same time the characteristic amide I band can overlap with the vibrational modes of organic or inorganic species, and it is recommended not to use it to build false-colour maps. Analogously, the intense *reststrahlen* band of carbonates in chalky layers can impede the detection of the amide II band. However, after the staining, this band appears more resolved. Hence, the best approach for the representation of protein layers from μ-FTIR data on this type of sample is the integration of amide II band.

5. Conclusions

SYPRO™ Ruby blot stain is a permanent luminescent metal chelate stain used in heritage science as an option for the identification of protein-based layers. For the first time, the impact of the staining procedure, but also of sample type and properties, has been documented in relation to the identification of protein in cultural heritage objects by external reflection μ-FTIR. The changes observed in the IR signals when spectra are collected in transmission, ATR and μ-FTIR mode confirmed that the staining material does not interact with protein. However, when the complexity of the sample is greater, other components of the multi-layered system play a significant role in the interaction with the staining solution, but also in protein detection. This is because they induce variations in position and intensity of the organic bands, as shown for all case studies presented. Additionally, the resin has a strong interference and usually makes the detection of protein more difficult. Further research on embedded samples might compare the influence of different embedding resins on the staining procedure.

The present investigation has shown that when the staining is performed first, followed by μ-FTIR, the contribution from amide I and II bands can be better resolved and the strategy used for protein mapping can be verified. However, it should be kept in mind that it also induces swelling of these layers, which affects the original morphology of the sample. This study also confirms that, despite the main IR bands of protein from glue are affected by spectral distortions when working in external reflection, their integration can still be used for a good estimation of protein distribution in multi-layer samples, both in terms of morphology and thickness, on mock-up samples and cross-sections from case studies. Further research could be conducted to determine the effectiveness of the protocol on other protein-based materials, such as egg, fish glue or casein.

CRediT authorship contribution statement

M. Botticelli: Conceptualization, Data curation, Investigation, Methodology, Validation, Writing – original draft. **V. Risdonne:** Conceptualization, Data curation, Investigation, Methodology, Writing – original draft. **C. Young:** Conceptualization, Supervision, Funding acquisition, Project administration, Writing – review & editing.

Declaration of Competing Interest

The authors declare that they have no known competing financial interests or personal relationships that could have appeared to influence the work reported in this paper.

Data availability

Data will be made available on request.

Acknowledgements

This project was supported by the UK Engineering and Physical Sciences Research Council [grant number EP/R033013/1], within the PISTACHIO (Photonic Imaging Strategies for Technical Art History And Conservation) project. Instruments were provided by the Arts and Humanities Research Council (AHRC) under Grant CapCo (Capability for Collections) "Equipping the Vision of Kelvin Hall" [grant number AH/V012398/1]. M.B. was also supported by a University of Glasgow, College of Arts Internal Investment fund. Mock-up samples belong to the Leverhulme research project 'The Biaxial Properties of Paintings on Canvas' [grant number F/624/C].

The authors express their gratitude to Dr. Mark Richter for supervising the staining and for the acquisition of data for samples S27 and S28. They are also grateful to the anonymous reviewers who helped us to improve the quality of the manuscript.

Appendix

Additional details are provided in this section for the historical samples subject of this study.

*Hector's farewell to Andromache (*Hunterian collection, University of Glasgow *GLAHA:44127)* was painted in Rome over a ten-year period (completed in 1756) by Gavin Hamilton (1723–1798). The painting has been examined by the Kelvin Centre for Conservation and Cultural Heritage Research within the PISTACHIO (Photonic Imaging Strategies For Technical Art History And Conservation) project and as part of its conservation. A preliminary observation of some samples showed an organic layer below the ground, most likely to be the size of the original preparation [37]. The characterization of its composition is of great relevance in the understanding of the painter's technique and sheds light on the possible influence from Italian painting traditions Hamilton so admired [38,39].

The Citizens Theatre paint frame. The Citizens Theatre in Glasgow features an original Victorian paint frame and related fly system, which is still used today to paint theatrical cloths (https://www.citz.co.uk). The frames and paint room walls show a complex superimposition of paint layers that records the backstage activities and aesthetic changes over two centuries. Characterising such a complex stratigraphy will help to identify historical phases in scenic art materiality and lead to a better understanding of distinctive trends and practices in theatrical scene painting [40].

Appendix A. Supplementary data

Supplementary data to this article can be found online at https://doi.org/10.1016/j.saa.2023.123067.

References

[1] E. Manzano, N. Navas, R. Checa-Moreno, L. Rodriguez-Simón, L.F. Capitán-Vallvey, Preliminary study of UV ageing process of proteinaceous paint binder by FT-IR and principal component analysis, Talanta. 77 (2009) 1724–1731, https://doi.org/10.1016/j.talanta.2008.10.014.

[2] M. Zuena, L. Baroni, V. Graziani, M. Iorio, S. Lins, M.A. Ricci, S. Ridolfi, L. Ruggiero, L. Tortora, L. Valbonetti, A. Sodo, The techniques and materials of a 16th century drawing by Giorgio Vasari: A multi-analytical investigation,

Microchem. J. 170 (2021) 106757, https://doi.org/10.1016/j.microc.2021.106757.
[3] A. Lluveras-Tenorio, S. Orsini, S. Pizzimenti, S. Del Seppia, M.P. Colombini, C. Duce, I. Bonaduce, Development of a GC–MS strategy for the determination of cross-linked proteins in 20th century paint tubes, Microchem. J. 170 (2021) 106633, https://doi.org/10.1016/j.microc.2021.106633.
[4] J. Walker, R. Hodgkins, B. Berrie, On the surface: Reflectance FTIR Spectroscopy in cultural heritage research, Microsc. Microanal. 27 (2021) 2800–2804, https://doi.org/10.1017/S1431927621009806.
[5] M. Vermeulen, K. Eremin, G. Rayner, K. Smith, T. Cavanaugh, A. McClelland, M. Walton, Micro reflectance imaging spectroscopy for pigment identification in painting cross sections, Microsc. Microanal. 27 (2021) 2806–2808, https://doi.org/10.1017/S1431927621009818.
[6] T.J. Bruno, Sampling Accessories for Infrared Spectrometry, Appl. Spectrosc. Rev. 34 (1999) 91–120, https://doi.org/10.1081/ASR-100100840.
[7] P. Peets, K. Kaupmees, S. Vahur, I. Leito, Reflectance FT-IR spectroscopy as a viable option for textile fiber identification, Herit. Sci. 7 (2019) 93, https://doi.org/10.1186/s40494-019-0337-z.
[8] M. Spring, C. Ricci, D.A. Peggie, S.G. Kazarian, ATR-FTIR imaging for the analysis of organic materials in paint cross sections: Case studies on paint samples from the national gallery, london, Anal. Bioanal. Chem. 392 (2008) 37–45, https://doi.org/10.1007/s00216-008-2092-y.
[9] S. Prati, I. Bonacini, G. Sciutto, A. Genty-Vincent, M. Cotte, M. Eveno, M. Menu, R. Mazzeo, ATR-FTIR microscopy in mapping mode for the study of verdigris and its secondary products, Appl. Phys. A. 122 (2016) 10, https://doi.org/10.1007/s00339-015-9519-z.
[10] C. Martin de Fonjaudran, A. Nevin, F. Piqué, S. Cather, Stratigraphic analysis of organic materials in wall painting samples using micro-FTIR attenuated total reflectance and a novel sample preparation technique, Anal. Bioanal. Chem. 392 (2008) 77–86, https://doi.org/10.1007/s00216-008-2111-z.
[11] S. Prati, F. Rosi, G. Sciutto, R. Mazzeo, D. Magrini, S. Sotiropoulou, M. Van Bos, Evaluation of the effect of six different paint cross section preparation methods on the performances of fourier transformed infrared microscopy in attenuated total reflection mode, Microchem. J. 103 (2012) 79–89, https://doi.org/10.1016/j.microc.2012.01.007.
[12] R. Mazzeo, E. Joseph, S. Prati, A. Millemaggi, Attenuated Total Reflection-Fourier transform infrared microspectroscopic mapping for the characterisation of paint cross-sections, Anal. Chim. Acta. 599 (2007) 107–117, https://doi.org/10.1016/j.aca.2007.07.076.
[13] S. Prati, G. Sciutto, E. Catelli, A. Ashashina, R. Mazzeo, Development of innovative embedding procedures for the analyses of paint cross sections in ATR FITR microscopy, Anal. Bioanal. Chem. 405 (2013) 895–905, https://doi.org/10.1007/s00216-012-6435-3.
[14] F. Rosi, L. Cartechini, D. Sali, C. Miliani, Recent trends in the application of fourier transform infrared (FT-IR) spectroscopy in heritage science: From micro: From non-invasive FT-IR, Phys. Sci. Rev. 4 (2019) 1–19, https://doi.org/10.1515/psr-2018-0006.
[15] J. Van Der Weerd, H. Brammer, J.J. Boon, R.M.A. Heeren, Fourier Transform Infrared microscopic imaging of an embedded paint cross-section, Appl. Spectrosc. 56 (2002) 275–283, https://doi.org/10.1366/0003702021954683.
[16] S. Prati, E. Joseph, G. Sciutto, R. Mazzeo, New advances in the application of FTIR microscopy and spectroscopy for the characterization of artistic materials, Acc. Chem. Res. 43 (2010) 792–801, https://doi.org/10.1021/ar900274f.
[17] Z.M. Khoshhesab, Reflectance IR Spectroscopy, in: T. Prof. Theophanides (Ed.), Infrared Spectrosc. - Mater. Sci. Eng. Technol., InTech, Rijeka, Croatia, 2012: pp. 233–244. doi:10.5772/37180.
[18] I. Arrizabalaga, O. Gómez-Laserna, J. Aramendia, G. Arana, J.M. Madariaga, Applicability of a diffuse reflectance infrared fourier transform handheld spectrometer to perform in situ analyses on cultural heritage materials, Spectrochim. Acta A Mol. Biomol. Spectrosc. 129 (2014) 259–267, https://doi.org/10.1016/j.saa.2014.03.096.
[19] J.S. Mills, R. White, The organic chemistry of museum objects, Butterworths & Co Ltd., London, 1987. doi:10.1016/C2009-0-63247-5.
[20] R.C. Nairn, Fluorescent protein tracing, E. & S. Livingstone, Edinburgh, 1964.
[21] I.C.A. Sandu, S. Schäfer, D. Magrini, S. Bracci, C.A. Roque, Cross-section and staining-based techniques for investigating organic materials in painted and polychrome works of art: A review, Microsc. Microanal. 18 (2012) 860–875, https://doi.org/10.1017/S1431927612000554.
[22] I.C.A. Sandu, A.C.A. Roque, P. Matteini, S. Schäfer, G. Agati, C.R. Correia, J.F.F. P. Viana, Fluorescence recognition of proteinaceous binders in works of art by a novel integrated system of investigation, Microsc. Res. Tech. 75 (2012) 316–324, https://doi.org/10.1002/jemt.21060.
[23] S. Schäfer, A luminescent metal chelate stain and its application protocol for the identification of proteinaceous binding media within paint cross sections, in: E. Emmerling, M. Kühlenthal, M. Richter (Eds.), Coloured Glazes Met, Leaf from Baroque Rococo, Anton Siegl Fachbuchhandlung, Munich, 2013, pp. 709–715.
[24] K. Berggren, T.H. Steinberg, W.M. Lauber, J.A. Carroll, M.F. Lopez, E. Chernokalskaya, L. Zieske, Z. Diwu, R.P. Haugland, W.F. Patton, A luminescent ruthenium complex for ultrasensitive detection of proteins immobilized on membrane supports, Anal. Biochem. 276 (1999) 129–143, https://doi.org/10.1006/abio.1999.4364.
[25] T. Rabilloud, J.-M. Strub, S. Luche, J.L. Girardet, A. van Dorsselaer, J. Lunardi, Ruthenium II tris (bathophenanthroline disulfonate), a powerful fluorescent stain for detection of proteins in gel with minimal interference in subsequent mass spectrometry analysis, Proteome. 1 (2000) 1–14, https://doi.org/10.1007/s102160000002.
[26] M. Bhalgat, Z. Diwu, R.P. Haugland, W.F. Patton, Luminescent protein stains containing transition metal complexes, WO 00/25139 (2000).
[27] T.H. Steinberg, R.P. Haugland, V.L. Singer, Applications of SYPRO orange and SYPRO red protein gel stains, Anal. Biochem. 239 (1996) 238–245, https://doi.org/10.1006/abio.1996.0320.
[28] SYPRO Ruby Blot stain webpage, (n.d.). https://www.thermofisher.com/order/catalog/product/S11791 (accessed December 15, 2021).
[29] T.H. Steinberg, L.J. Jones, R.P. Haugland, V.L. Singer, SYPRO orange and SYPRO red protein gel stains: One-step fluorescent staining of denaturing gels for detection of nanogram levels of protein, Anal. Biochem. 239 (1996) 223–237, https://doi.org/10.1006/abio.1996.0319.
[30] F. Rosi, A. Federici, B.G. Brunetti, A. Sgamellotti, S. Clementi, C. Miliani, Multivariate chemical mapping of pigments and binders in easel painting cross-sections by micro IR reflection spectroscopy, Anal. Bioanal. Chem. 399 (2011) 3133–3145, https://doi.org/10.1007/s00216-010-4239-x.
[31] M. Derrick, D. Stulick, J. Landry, Infrared Spectroscopy in Conservation Science, J. Paul Getty Trust, Los Angeles, 1999.
[32] A. Barth, C. Zscherp, What vibrations tell about proteins, Q. Rev. Biophys. 35 (2002) 369–430, https://doi.org/10.1017/S0033583502003815.
[33] A. Barth, Infrared spectroscopy of proteins, Biochim. Biophys. Acta - Bioenerg. 1767 (2007) 1073–1101, https://doi.org/10.1016/j.bbabio.2007.06.004.
[34] C. Invernizzi, T. Rovetta, M. Licchelli, M. Malagodi, Mid and near-infrared reflection spectral database of natural organic materials in the cultural heritage field, Int. J. Anal. Chem. 2018 (2018), https://doi.org/10.1155/2018/7823248.
[35] L. Monico, F. Rosi, C. Miliani, A. Daveri, B.G. Brunetti, Non-invasive identification of metal-oxalate complexes on polychrome artwork surfaces by reflection mid-infrared spectroscopy, Spectrochim. Acta A Mol. Biomol. Spectrosc. 116 (2013) 270–280, https://doi.org/10.1016/j.saa.2013.06.084.
[36] C. Miliani, F. Rosi, I. Borgia, P. Benedetti, B.G. Brunetti, A. Sgamellotti, Fiber-optic fourier transform mid-infrared reflectance spectroscopy: A suitable technique for in Situ studies of mural paintings, Appl. Spectrosc. 61 (2007) 293–299, https://doi.org/10.1366/000370207780220840.
[37] D.E. Beynon-Gray, Gavin Hamilton's methods and materials: Technical analysis of Hector's farewell to Andromache, University of Glasgow, 2021.
[38] B. Cassidy, The Life Letters of Gavin Hamilton (1723–1798): Artist & Art dealer in eighteenth-century Rome, Harvey Miller Publishers, London, 2011.
[39] G. D'Anna, S. Marconi, C. Merucci, M.L. Papini, L. Traversi, Preparazioni e imprimiture dei dipinti su tavola e tela: materiali, metodi e storia, in: C. Maltese (Ed.), Prep. e Finit. Delle Opere Pittoriche, Mursia, Milano, 1993: pp. 11–38.
[40] C. Young, The changing role and status of scenic artists in England, in: Setting The Scene, Archetype Publications Ltd, London, 2013: pp. 99–107.